

Article

A Finite Element Analysis of a Tooth-Supported 3D-Printed Surgical Guide without Metallic Sleeves for Dental Implant Insertion

Ionut Gabriel Ghionea ¹, Oana Elena Burlacu Vatamanu ^{2,*}, Ana Maria Cristescu ³, Mihai David ⁴,
Izabela Cristina Stancu ⁵, Cristian Butnarusu ⁶ and Corina Marilena Cristache ^{4,*}

¹ Manufacturing Engineering Department, Faculty of Industrial Engineering and Robotics, National University of Science and Technology Politehnica Bucharest, 313 Splaiul Independenței, 060042 Bucharest, Romania; gabriel.ghionea@upb.ro

² Doctoral School, “Carol Davila” University of Medicine and Pharmacy, 37 Dionisie Lupu Street, 020021 Bucharest, Romania

³ Faculty of Medical Engineering, National University of Science and Technology Politehnica Bucharest, 1-7 Gh Polizu Street, 011061 Bucharest, Romania

⁴ Department of Dental Techniques, “Carol Davila” University of Medicine and Pharmacy, 8, Eroii Sanitari Blvd., 050474 Bucharest, Romania

⁵ Advanced Polymer Materials Group, Faculty of Chemical Engineering and Biotechnologies, National University of Science and Technology Politehnica Bucharest, 1-7 Gh Polizu Street, 011061 Bucharest, Romania

⁶ Megagen Dental Laboratory, 38 Delea Nouă Street, 030925 Bucharest, Romania; cristian.butnarusu@gmail.com

* Correspondence: oana-elena.burlacu-vatamanu@drd.umfcd.ro (O.E.B.V.); corina.cristache@umfcd.ro (C.M.C.)

Abstract: Static guided surgery for dental implant insertion is a well-documented procedure requiring the manufacturing of a custom-made surgical guide, either teeth-supported, mucosal-supported, bone-supported, or mixed (teeth-mucosal-supported), depending on the clinical situation. The guidance of the surgical drills during implant bed preparation could be undertaken using a sequence of different diameters of metal drill sleeves or, with the sleeves incorporated in the surgical guide, shank-modified drills, both clinically accepted and used with good results. Despite the great number of advantages associated with the use of guided surgery, one of the major risks is guide fracture during drilling for implant bed preparation. Therefore, the aim of the present study was to evaluate the surgical guides without metal sleeves and to simulate, with the aid of Finite Element Analysis (FEA), the use of such dentally supported guides for implant insertion. The FEA is performed in CATIA v5 software after defining the surgical guide mesh material and bone properties. A maximum stress of 6.92 MPa appeared on the guide at the special built-in window meant to allow cooling during drilling, and the maximum value of the guide displacement during drilling simulation was 0.002 mm. Taking into consideration the limits of the current research, the designed tooth-supported surgical guide can withstand the forces occurring during the surgery, even in denser bone, without the risk of fracture.

Keywords: surgical guide; finite element analysis; 3D model preparation; mandible; drilling process relations; guided dental implants insertion



Citation: Ghionea, I.G.; Vatamanu, O.E.B.; Cristescu, A.M.; David, M.; Stancu, I.C.; Butnarusu, C.; Cristache, C.M. A Finite Element Analysis of a Tooth-Supported 3D-Printed Surgical Guide without Metallic Sleeves for Dental Implant Insertion. *Appl. Sci.* **2023**, *13*, 9975. <https://doi.org/10.3390/app13179975>

Academic Editor: Luca Testarelli

Received: 16 August 2023

Revised: 1 September 2023

Accepted: 2 September 2023

Published: 4 September 2023



Copyright: © 2023 by the authors. Licensee MDPI, Basel, Switzerland. This article is an open access article distributed under the terms and conditions of the Creative Commons Attribution (CC BY) license (<https://creativecommons.org/licenses/by/4.0/>).

1. Introduction

In the last few years, digital dentistry has become a part of everyday practice for dental professionals, and with the aid of intraoral scanners (IOS), facial scanners, Cone Beam Computed Tomography (CBCT), a virtual patient could be created to facilitate better treatment planning, communications between dental specialists and dental technicians, and a better understanding of patients expectations [1,2]. In complex cases such as the rehabilitation of patients with failing teeth/failing restorations, digital planning can be achieved based on 3D images obtained through IOS (.stl—standard tessellation language

files), facial scanning (.obj—Wavefront 3D Object files), and DICOM (Digital Imaging and Communications in Medicine) files from CBCT, merged in dedicated software. A wax-up of the provisional restoration will be designed based on the available data, and prosthetically driven implant insertion can be planned according to the provisional restoration and the existing residual bone. The planned implant positioning is then transferred to the surgical field using a 3D-printed or milled surgical guide [3].

In the digitalization era, not only complicated cases are planned and solved in full digital protocol. Nowadays, all implant insertions can be fully digitally planned in order to achieve immediate provisional restoration and guided insertion to increase predictability [4].

In addition to a rigorous treatment plan approved by the surgical and restorative teams and agreed upon by the patient, one important step is transposing the planned implant position into the surgical setting. This can be undertaken either statically, using a surgical guide, or dynamically, assisted by a navigation device equipped with an optical tracking system [4,5]. Static-guided surgery is preferred in many cases due to its predictability. The guide is easier and faster to manufacture and apply in any dental clinic and involves low costs and a minimally invasive surgical procedure for the patient. It also requires less initial investment in sophisticated, expensive equipment. In addition to higher investments in equipment, dynamically guided implant insertion requires a longer learning curve for the surgeon [6,7].

Static guided surgery is a well-documented procedure requiring the manufacturing of a custom-made surgical guide, either teeth-supported, mucosal, bone-supported, or mixed (teeth-mucosal-supported), depending on the clinical situation. Additionally, the guidance of the surgical drills during implant bed preparation could be undertaken using a sequence of different diameters of drill sleeves or, less complicated, sleeveless, with the sleeves incorporated in the surgical guide and shank-modified drills [5,8], both clinically accepted and used with good results [9]. For the surgical guides with metal sleeves, the body of the guide is manufactured separately, and the sleeves with various internal diameters are prefabricated, in contrast to the metal-sleeve-free guides, where the design of the surgical guide includes the sleeves so that they can be obtained simultaneously. According to Schneider et al., a lower tolerance of surgical instruments and subsequently a reduced amount of lateral movement of the drills during osteotomy were observed with the use of guides without any metal sleeves [10]. Other advantages, such as the use of in-office printers for guide manufacturing [11], a clinically acceptable accuracy of dental implant insertion [5,12,13], and better drill cooling for avoiding bone necrosis due to the special built-in window, increased the popularity of sleeve-incorporated resin surgical guides [14].

The accuracy of the reproduction of the planned implant position is mandatory for a successful treatment and the avoidance of complications. In spite of the high degree of predictability of the surgical guides reported in the literature, some complications, such as guide fracture, could occur [15,16]. Few studies are focused on analyzing the mechanical behavior of full resin surgical guides and stress distribution during implant surgery to improving their design and strength [17,18], while they are custom-created for each individual patient.

Finite Element Analysis (FEA) is a numerical method for stress and deformation analysis of a given and complex geometry, simulated under various physical conditions, commonly used nowadays in medical and dental fields. For analysis, the shape is discretized into many small elements, so-called finite elements, coupled at the corners through nodes. Each element is a tetrahedron, with its sides having different lengths. In a complex structure, each face, side, and node are shared with those of an adjacent element. For each individual element, its mechanical behavior can be described as the function of the displacement of the nodes. When certain loading conditions and specific restraints are applied to the whole 3D model/structure, and the specific characteristics of the material are provided, the behavior of this model can be obtained, and the stress and strain can be computed on the desired parts of the shape. The accuracy of the results is determined by the total number of elements used for the model (also called discretization of the model in finite

elements), as well as by the type of the network mesh (linear or parabolic) [19,20]. Each setting (3D model complexity, finite element type, discretization level, structure loading mode, FEA computation accuracy) influences the analysis results and their interpretation.

The objective of the present study is to develop surgical guides without metal sleeves (with incorporated sleeves) and to explore and simulate through FEA the use of such a dentally supported guide for dental implant insertion. Additionally, the behavior of the guide's 3D model is evaluated by simulation for design validation and improvement proposals. The present study is structured in two parts. Firstly, the manufacturing workflow of surgical guides with sleeves incorporated (without metal sleeves/sleeveless) is discussed. In the second part, a FEA and methodology are applied to a surgical guide for simulating the implant bed preparation.

2. Materials and Methods

2.1. Workflow for Surgical Guide Design and Manufacturing

The manufacturing of a surgical guide for dental implant insertion is based on a set of data collected from the patient. These data are imported into a planning and design software; the future restoration is planned as a virtual wax-up, and based on this and available bone volume, a dental implant is selected from the software's library and its position is set based on the final planned restoration. The surgical guide is custom designed in accordance with the planned implant position using reverse engineering. Depending on the type of support (dental, mucosal, or mixed), additional temporary fixation systems are also designed to improve guide retention.

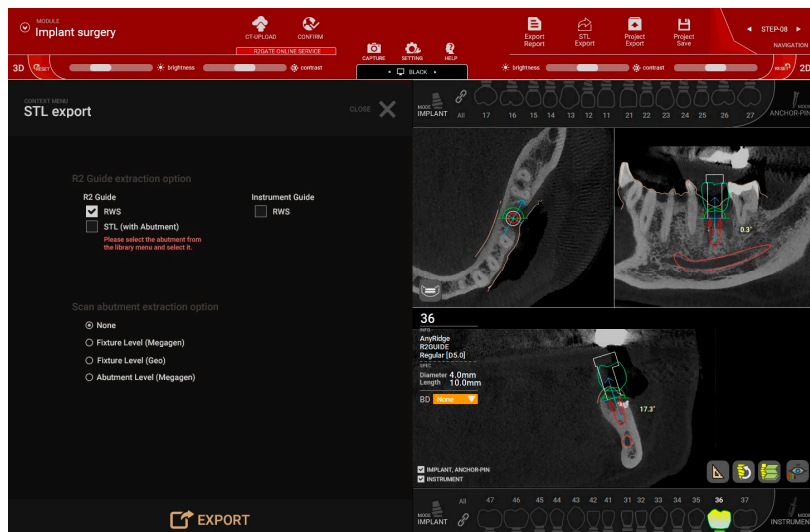
Digital impressions or scanned analog models obtained from analog impressions, cone-beam computed tomography (CBCT), and digital wax-ups of the future restoration are the main data utilized in dental implant positioning planning and static surgical design.

There are several pieces of software used for the planning and design of surgical guides, such as Exoplan (Exocad GmbH, Darmstadt, Germany), R2Gate™ (MegaGen, Daegu, Republic of Korea), Blue Sky Bio (LLC, Libertyville, IL, USA), Simplant Pro™ (Dentsply, Sweden), ImplantStudio (3Shape, Copenhagen, Denmark), and so on.

The steps of surgical guide planning using R2Gate software, version 2.0, are presented in Figure 1.

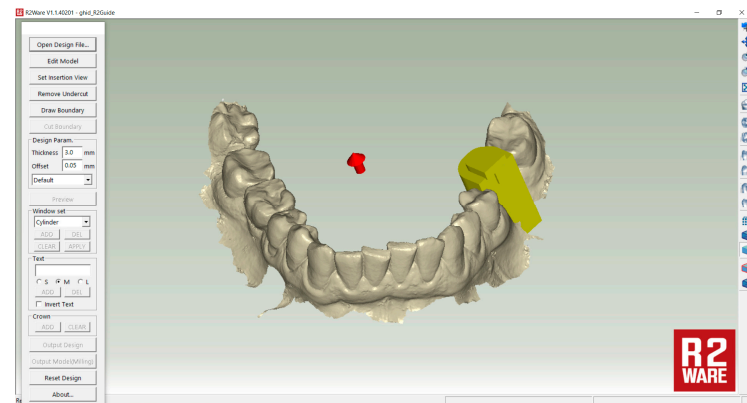
The planned implant insertion is exported as .rws file (RimWorld game save file) or as a .stl file (stereolithography—a popular 3D printing technology). R2Ware version 1.1.40201 software uses .rws files for the design of the surgical guide with incorporated sleeves, and the main steps are: (1) remove undercuts; (2) draw boundaries; (3) cut boundaries; (4) set parameters (thickness of the guide and offset—the space between the inner surface of the guide and the surface of the model); (5) window set (for inspecting windows used to ensure that surgical guides fit well on neighboring teeth); and (6) text (for writing the patient's name on the external surface of the guide) (Figure 2a,b). The designed guide (Figure 2c) is usually manufactured with the aid of a 3D printer (additive manufacturing) or, less often, by milling in an acrylic blank (subtractive manufacturing). Due to its ability to reproduce complex structures at reduced cost and reduce material waste, additive manufacturing is the most popular method [21,22]. The full resin surgical guide is printed using E-Guide Resin (EnvisionTEC GmbH, Gladbeck, Germany) with the Digital Light Processing (DLP) technique, and its fit is checked on the patient's model (Figure 2d) before using it for implant surgery.

The same workflow is followed for planning, designing, and manufacturing surgical guides with mucosal or mixed support. Additional transversal pins are required, in certain cases, for guide stabilization.

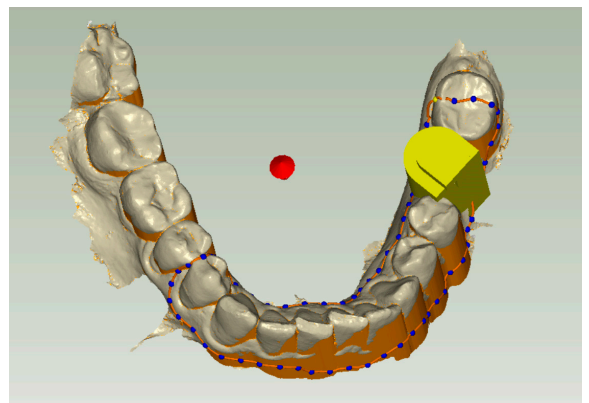


(g)

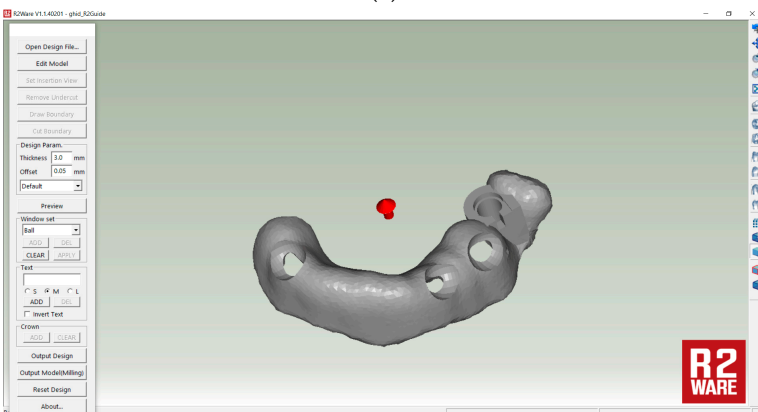
Figure 1. Surgical guide design in R2Gate™ software, version 2.0: (a) DICOM files from CBCT and .stl files of the patient’s corresponding dental arch impression are imported in the software, and a three-point matching is performed; (b) a second 3D manual matching of CBCT with the digital model is undertaken; (c) design of the digital wax-up; (d) for dental implant insertion in the mandible, one extra step, alveolar nerve tracing, is required; (e) selecting the adequate implant and 3D positioning panning according to the final prosthetic restoration and the existing width and height of the bone; (f) when planning is performed and approved, the R2Gate corresponding drill core is selected and the window is positioned on the buccal side; (g) the planned implant position is exported as .rws file.



(a)



(b)



(c)



(d)

Figure 2. Guide design in R2Ware software, version 1.1.40201: (a) the .rws file of the planning im-plant insertion is imported in the software; (b) the undercuts are removed and the limits of the

surgical guide are traced using the option “draw boundary”; (c) the thickness of the guide is set at 3 mm (default) and the offset at 0.05 mm, and three inspecting windows are designed to check the perfect fit on the neighboring teeth; (d) the surgical guide is 3D printed in clear, transparent E-Guide Resin, postprocessed, and its fit is checked on the 3D printed model of the patient’s dental arch.

2.2. Mesh Geometry Refinement for Finite Element Analysis (FEA)

The .stl file of the surgical guide, obtained following the previously mentioned procedures, contains a surface of medium to high complexity, specific to each patient. In the .stl format, each file is made up of a series of linked triangles that describe the surface geometry of a 3D model or object. The network of triangles is denser in certain sensitive areas of the object, and therefore, it can approximate it with very good precision.

The surface (in fact, it is a mesh surface) has area properties; it can be divided into several individual areas for checking (it works faster on smaller areas); it is delimited by numerous edges; but it has no volume property, so it cannot be assigned material properties. Thus, the surface in .stl file must be transformed into a solid object by filling the inner cavity of the complex mesh surface. To prepare it for transformation into a solid object, the user must check if the respective mesh surface is orientable.

It is known that the orientation of a mesh surface is given by the cyclic order of its vertices. Thus, it is considered that a mesh surface is orientable if all its faces point outside. Additionally, the user should check the mesh for self-intersection. This is a situation where a part of a mesh surface collides/interferes with another part of itself (two mesh elements intersect each other).

Many problems affect the integrity of the mesh surface and make it unusable for most applications. These checks should always be considered before initiating a solid transformation and simulation because the mesh integrity has a crucial influence on the accuracy of the results. As an example of the check process, Yamakawa and Shimada [23] describe a computational method for identifying and removing self-intersections of a triangular mesh.

The open-source software MeshLab (EUIPO trademark, distributed under CC BY-SA 4.0) was used to optimize and clean the designed .stl mesh [24].

2.3. Finite Element Analysis on a Tooth-Supported Surgical Guide for Simulating Implant Bed Preparation in the Mandible Bone

In order to prepare the FEA, it is necessary to transform the mesh surface into a solid object using the CATIA v5 program (Computer Aided Three-dimensional Interactive Applications, France). The working methodology is inspired by the theoretical and applied research presented by Leordean et al. [25], and the whole process, which contains several important steps, is presented in detail in a YouTube video available at the following link: (https://www.youtube.com/watch?v=H6_XfjD3yqs), accessed on 31 August 2023 [26].

In the first step, the .stl file is opened and the integrity of the whole mesh surface is visually checked. However, this is just a first and simple check; CATIA v5 will verify the surface and then the solid each time the user opens or tries to work on the 3D model.

From the DMU Optimizer workbench, the Offset tool is used, which creates a new surface superimposed on the initial surface (offset value = 0 mm), according to Figure 3. This newly obtained surface is saved as a .model file, and it is easily recognized by the program in the following steps.

Figure 3 also shows the network of triangles; the denser it is, the more precise the surface, but the processing/simulation time also increase significantly. By default, this step contains a check of the initial surface in the .stl file. If the integrity of this initial surface had been affected in any way, the offset operation would not have been possible.

In the second step, with the help of the Part Design workbench, the user opens the .model file. It contains a series of small patch surfaces formed by several triangular elements of the initial surface. This is, therefore, a first simplification and union of the individual elements of the mesh surface (Figure 4). All these Surface.x components, as represented in

the specification tree in Figure 4, are joined into a single surface with the help of the Join tool. Its dialog box contains several options for checking and simplifying the final surface. Thus, the program checks for tangency and connexity issues while trying to simplify the resulting surface.

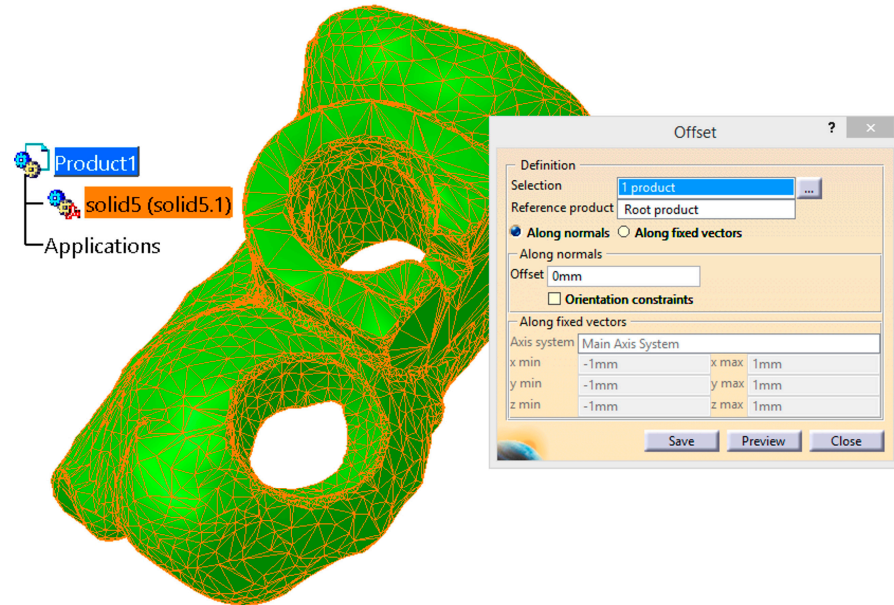


Figure 3. Initial mesh surface of the guide from the .stl file while it is offset to create a new surface/model in order to be recognized by the CATIA v5 program.

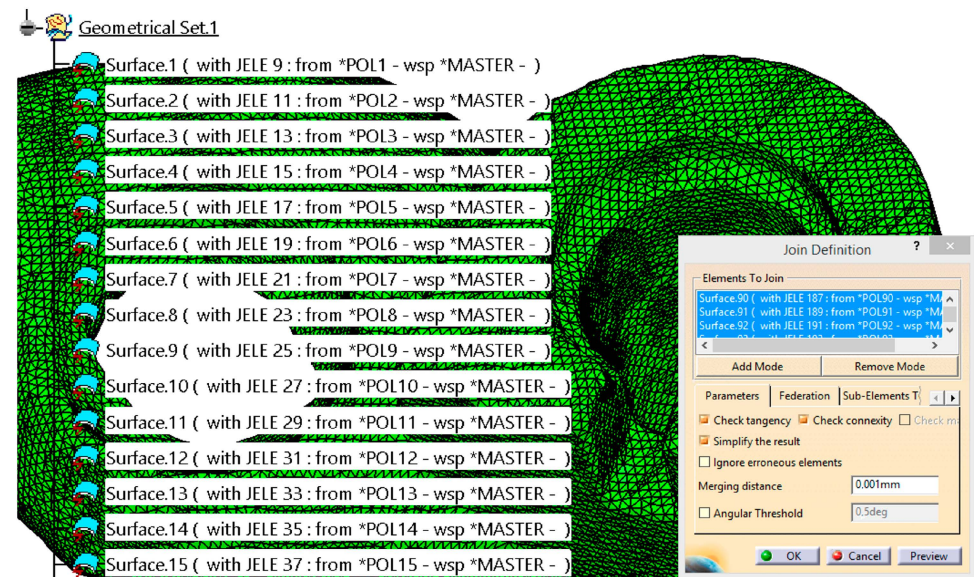


Figure 4. Joining the surface elements while simplifying the resulted surface and checking for tangency and connexity issues.

While creating the .model file, the user decides if it is convenient for the FEA. Most of the time, it is necessary and recommended to reduce the number of triangle elements with the help of the Simplification tool.

For example, the number of triangles in the guide model studied in this paper was reduced from 82,180 to 2818. This decision leads to a much faster FEA, but also to easy manipulation of the model between the workbenches of the CATIA v5 program. The applied simplification, although substantial, does not produce significant changes in the area and volume properties of the guide.

In the third step, once the mesh surface model has been created, verified, and simplified, the Close Surface tool is applied, and a solid object is obtained by filling the surface created according to Figure 4. This solid object can receive material properties and may be involved in a finite element analysis.

Numerous constraint conditions are established for certain surfaces at the base of the guide to simulate its positioning/fixing on neighboring teeth; other surfaces are loaded with forces and moments due to the contact between the guide and the body of the drill.

Finite element analysis considers the worst-case scenario when the tapered shank of the drill is in contact with the corresponding surfaces of the guide.

The FEA is performed in CATIA v5 after defining the following elements:

- .stl mesh of a tooth-supported surgical guide reduced to a limited extent at the neighboring teeth, optimized, and cleaned in the open-source software MeshLab [24];
- Material properties for surgical guide manufacturing via DLP 3D printing: E-Guide Resin (EnvisionTEC GmbH, Gladbeck, Germany): Flexural strength = 79–86 MPa; Poisson Ratio = 0.3; Density = 1.12 g/cm³; Young Modulus = Tensile Modulus = Elastic Modulus = 2.6 GPa = 2600 MPa;
- Mandibular bone properties [27–29]: Density = 1.2 g/cm³; Young Modulus = 15–30 GPa; Poisson Ratio = 0.3; Hardness (HB) = 56; Flexural strength = 70–150 MPa;
- The mesh used to discretize the guide's 3D model is composed of 90,217 finite elements (tetrahedrons), connected by 145,237 nodes.

The 3D model is discretized using a minimum mesh size of 0.5 mm and an absolute sag (minimum distance between nodes and boundary) of 0.2 mm. For higher accuracy in the complex mesh, the finite element type is parabolic. An additional refinement of the mesh network with a smaller size of the finite elements is not necessary and does not offer important changes to the analysis results, but it would significantly increase the resources required for the FEM computations [30].

Based on the specialized literature [31,32] and on several clinical tests/protocols recommended by the manufacturers of dental implants, the authors propose relations and values for the most important parameters used in the process of drilling the mandible bone. Some of these parameters and their coefficients are experimentally determined; they have moderate values, which ensure a safe drilling of the bone. The authors recommend using higher values with caution for the feed ratio speed, cutting speed, and axial cutting force. The moderate/safe values are because the mandible bone differs from one patient to another depending on gender, age, various health conditions, and also on the drilling protocol.

Thus, the parameters of the drilling regime with a $d = \text{Ø}2$ mm drill are presented:

Feed— f (mm/rev)—the distance that a drill advances into the bone in one complete rotation,

$$f = K_f \times C_f \times d^{0.6}, \text{ mm/rev},$$

$$f = 0.85 \times 0.055 \times 2^{0.6} = 0.071 \text{ mm/rev},$$

where K_f is a correction coefficient depending on the hole depth h and its diameter $h > 3d$ ($10 \text{ mm} > 3 \times 2 \text{ mm}$); $K_f = 0.85$; C_f is the feed coefficient based on the bone hardness and drilling precision; $C_f = 0.055$; d is the drill diameter.

Feed ratio speed— V_f (mm/min)

$$V_f = f \cdot n, \text{ mm/min},$$

$$V_{f750} = 0.071 \times 750 = 53.3 \text{ mm/min},$$

$$V_{f1200} = 0.071 \times 1200 = 85.2 \text{ mm/min},$$

where n is the rotational speed required for drilling (values considered between 750 rev/min and 1200 rev/min depending on the bone condition and on the area where the hole will be positioned). We noticed that the maximum safe rotational speed should be up to 1800–2000 rev/min.

Cutting speed— V_c (m/min)

$$V_c = \pi \times d \times n/1000, \text{ mm/min},$$

$$V_{c750} = \pi \times 2 \times 750/1000 = 4.71 \text{ m/min},$$

$$V_{c1200} = \pi \times 2 \times 1200/1000 = 7.53 \text{ m/min}.$$

Axial cutting force— F_{fw} (N)

$F_{fw} = C_{F1} \cdot d^{xF} \cdot f^{yF} \cdot HB^{nF} \cdot K_F$, (N), where C_{F1} is experimentally determined based on the bone hardness, $C_{F1} = 1.6$; x^F and y^F are experimentally determined correction coefficients depending on the hardness of the mandible bone and on the drilling conditions (the drill tool is guided or not, the drilling process is with or without cooling), $x^F = 1$, $y^F = 0.7$; $f = 0.071$ mm/rev; HB —mean value of the mandible bone hardness, $HB = 56$ HB; n^F is an experimentally determined coefficient that depends on the drill's type and on the hardness of the mandible bone, $n^F = 0.75$; K_F is a correction coefficient of the drilling force, determined by: $K_F = K_{aF} \times K_{faF} \times K_{\chi F} \times K_{\eta F}$, where: K_{aF} is a correction coefficient depending on the sharpening method of the drill, $K_{aF} = 1$; K_{faF} is a correction coefficient experimentally determined based on the manual advancement of the drill, $K_{faF} = 0.97$; $K_{\chi F}$ is a correction coefficient depending on the value of the angle of the drill tip ($2\chi^0$), $K_{\chi F} = 0.98$; $K_{\eta F}$ is a correction coefficient depending on the relative thickness of the drill core η , and its diameter, $d = \varnothing 2$ mm, $\eta = 0.18$, $K_{\eta F} = 1.19$.

So, $K_F = 1 \times 0.97 \times 0.98 \times 1.19 = 1.13$, and $F_{fw} = 1.6 \times 2^1 \times 0.071^{0.7} \times 56^{0.75} \times 1.13 = 11.62$ N

Cutting torque— M_W (N·m)

$M_W = C_{M1} \times d^{xM} \times f^{yM} \times HB^{nM} \times K_{\eta M}$, N·m, where C_{M1} is a coefficient experimentally determined based on the bone hardness, $C_{M1} = 0.0163$; $d = \varnothing 2$ mm; x^M and y^M are correction coefficients experimentally determined based on the bone hardness and drilling conditions (guided, with/without cooling), $x^M = 1.3$, $y^M = 0.93$; $HB = 56$ HB; n^M is a coefficient experimentally determined based on the drill's type and on the bone hardness, $n^M = 0.54$; $K_{\eta M}$ is the correction coefficient of the cutting torque, $K_{\eta M} = 1.1$

$M_W = 0.0163 \times 2^{1.3} \times 0.071^{0.93} \times 56^{0.54} \times 1.1 = 0.033$ N·m

Total cutting power— P_c (W)

$P_c = P_F + P_M$, (W), where P_F is the power derived from the feed and P_M is the power derived from the cutting torque.

$P_c = V_f \times F_{fw} + M_W \times n \times 2\pi/60 = 0.02 + 4.14 = 4.16$ W.

At the base of the guide, certain areas are carefully established, considering that they are in contact with neighboring teeth, and specific constraints are applied to fix the guide. The areas fixed in this manner will not present displacements following the FEA simulation (Figure 5).

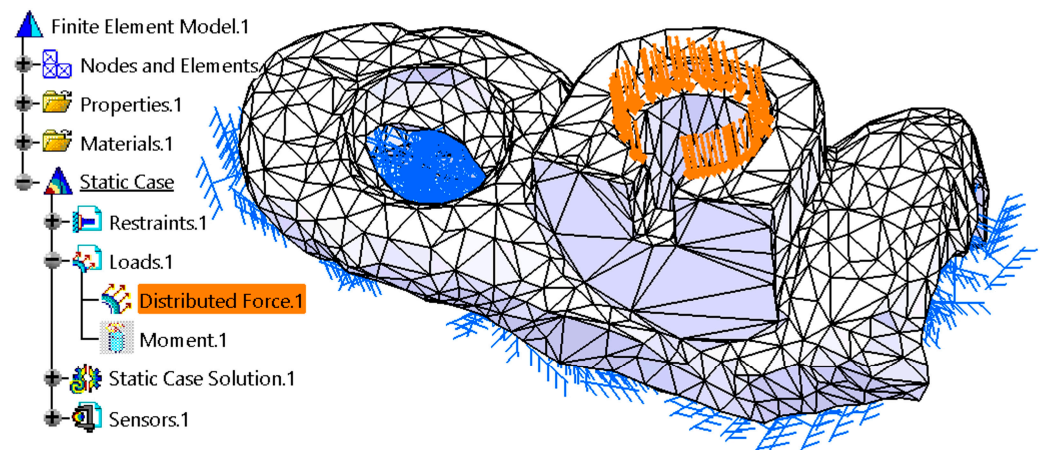


Figure 5. Applying restraints and loads to the solid 3D model of the guide.

The main load of the guide is given by the axial cutting force $F_{fw} = 11.62$ N, arranged on the surface of the guide (Figure 5) to limit the movement of the drill in the process of drilling into the mandible bone. Additionally, on the inner cylindrical surface of the main hole of the guide is applied a cutting torque equal to 10% of M_W . The value of 10% is average and recommended. This value depends a lot on the quality of the surfaces of the drill and the guide, but also on the way the surgeon manipulates the drill so that its axis coincides, as much as possible, with the axis of the guide hole. The establishment of this

value is based not only on research and recommendations found in the literature [31,32], but also on many observations and practical determinations.

Thus, in clinical practice, we observed that the cutting torque that is lost by friction with the guide is about 10–20% of the calculated M_W . This cutting torque was lost by friction loads on the cylindrical surface of the guide's main hole.

These conditions that constrain and load the guide are relatively complex, so the finite element analysis requires important hardware resources. The simulation was undertaken on a 9th generation i7 computer with 3.6 GHz, 32 Gb of RAM, a 1Tb SSD, and Windows 10.

3. Results

To showcase the use of a teeth-supported type of sleeveless guide during the surgical procedures for implant bed preparation and dental implant insertion, a simulation of the procedure is displayed in Figure 6. For example, for the insertion of a $\text{\O}4$ mm diameter and 10 mm length AnyRidge™ (MegaGen, Daegu, Republic of Korea) dental implant, the following guide stop drill sequence is recommended: 2 mm \times 7 mm, 2 mm \times 8.5 mm, 2 mm \times 10 mm; 2.5 mm \times 10 mm; 2.8 mm \times 10 mm; 3.3 mm \times 10 mm; and 3.8 mm \times 10 mm. The drilling protocol is adjusted according to the crestal bone density to increase the implant's primary stability [8].

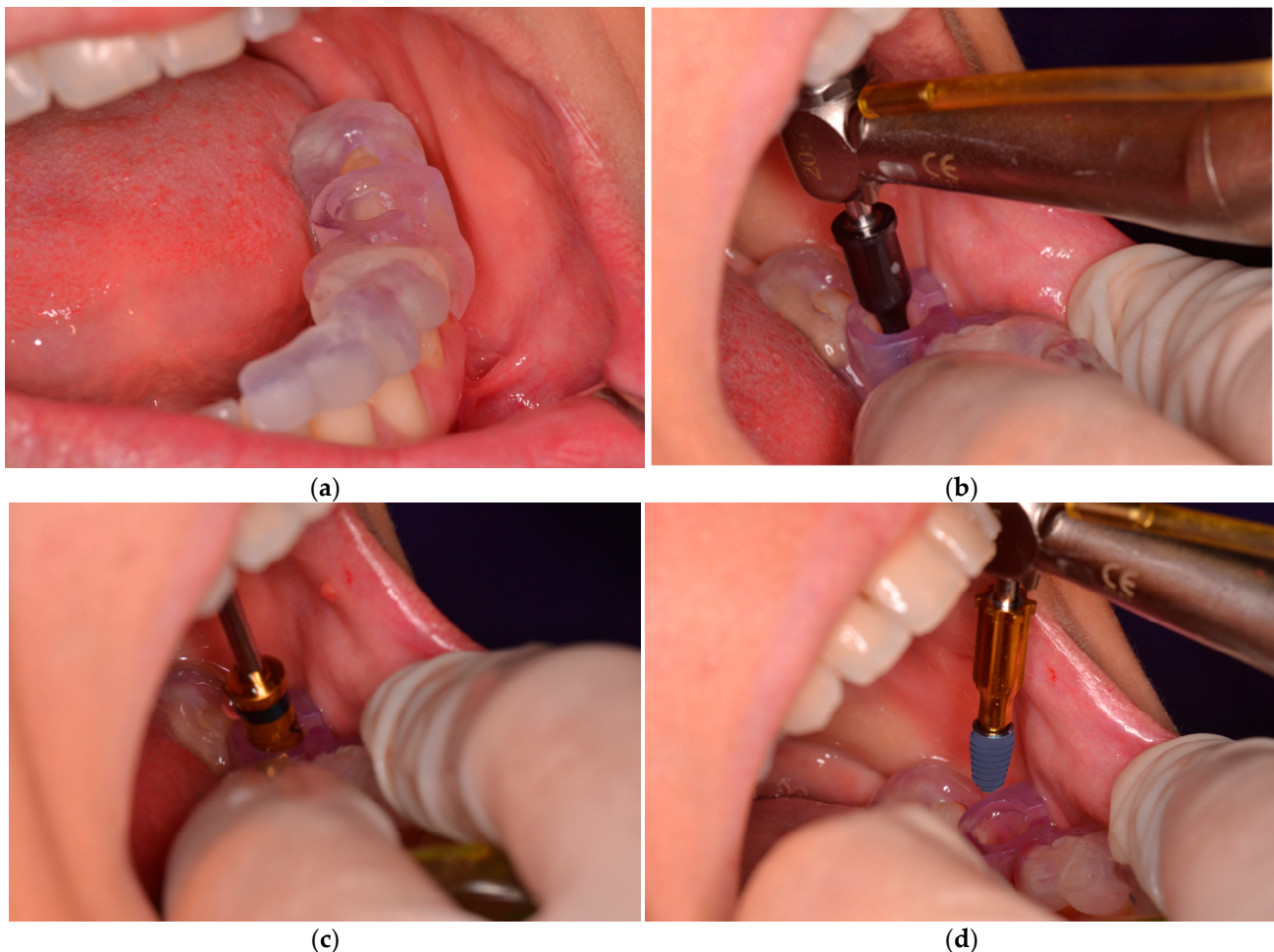


Figure 6. Representative digital images suggestive of flapless implant bed preparation and insertion with the aid of the surgical guide, without metallic sleeves: (a) the guide is placed over the remaining natural teeth (tooth-supported guide type); (b) an initial drill is needed to initial the path in the cortical bone; (c) the implant osteotomy has to be prepared using the guide stop drills in a successive order based on drill diameter and length; (d) guided dental implant insertion.

The .stl file of a tooth-supported mandibular surgical guide, designed in R2Ware software and reduced, optimized, and cleaned in the open-source software MeshLab, was used for FEA in CATIA v5 software. The quality of the finite elements and the overall analyzed guide was very good (99.98%), meaning that the solid 3D model obtained from the designed guide was correct and consistent. This value was obtained by using a CATIA v5 program tool called Quality Analysis. The Quality Analysis dialog box appears with a default list of criteria that are taken into account for the mesh quality check and for the mesh optimization. Figure 7 presents the discretization of the guide's model, revealing that its mesh is very complex.

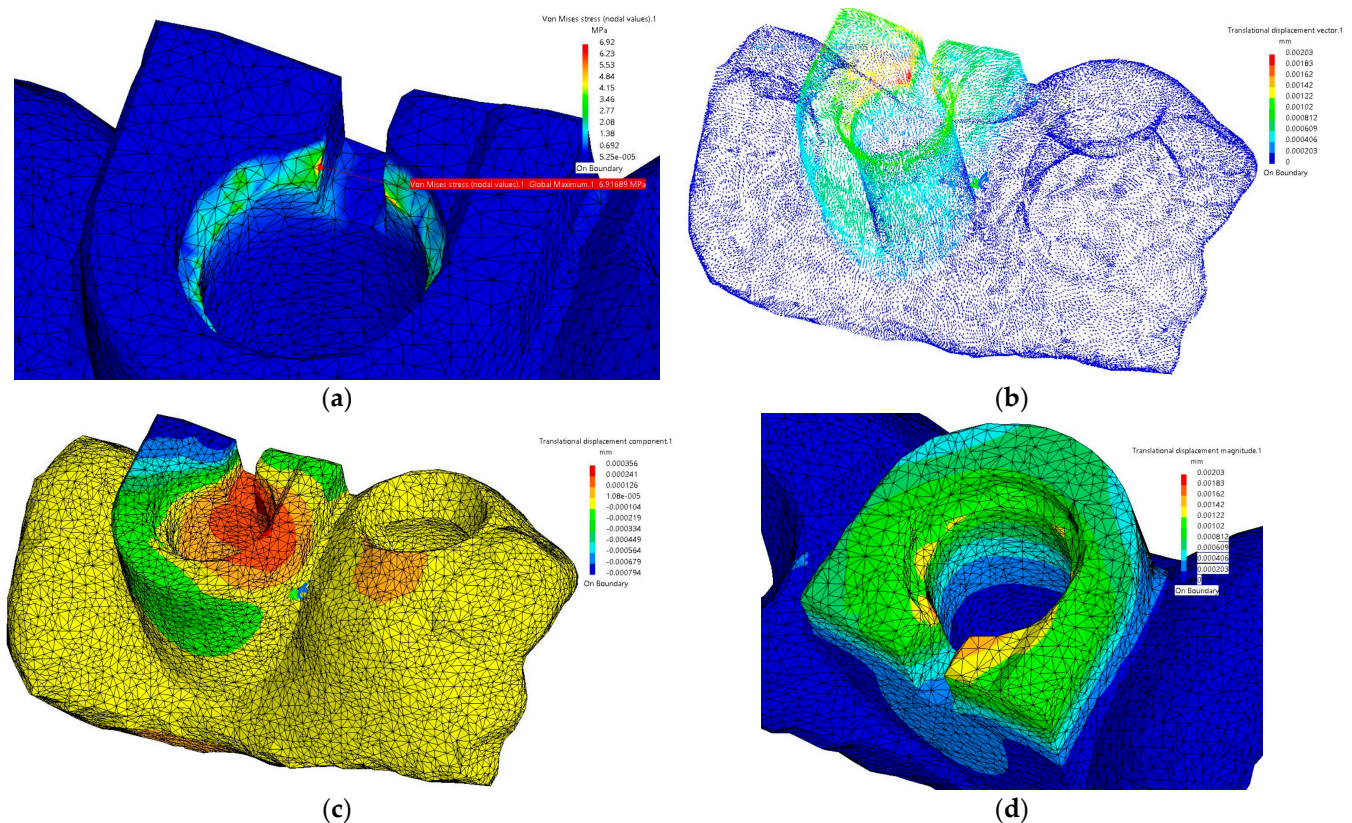


Figure 7. Results of the finite element analysis: (a) location and values of the maximum stress; (b) displacements of the guide and their maximum value; (c,d) propagation of the displacements showing the most critical areas.

The FEA was also a complex one: the program identified and took over 435,711 degrees of freedom (DOF).

In the present study, the use of the first drill ($\varnothing 2$ mm diameter) \times 10 mm length was simulated for implant bed preparation in the mandibular bone. Von Mises stresses, determining whether the material and the design of the surgical guide will lead to guide fracture, were determined.

As is obvious, the most stressed area is on the cylindrical surface of the main hole of the guide, through which the drill passes. Since the moment due to the friction between the drill shank and the guide is very small (10% of M_w), its influence is not so important.

The axial force is the one that, at a given moment, loads the tapered area present at the entrance to the main hole of the guide and produces a maximum stress of 6.92 MPa (Figure 7a). This stress value is not low but normal, considering that the flexural strength of the guide's material is approximately 80–86 MPa. As a consequence, the first remark is that there is no danger of the guide failing/breaking, provided that it has no manufacturing defects and is correctly fixed on the teeth so that it does not vibrate in the drilling process.

The areas with maximum stresses appear on the guide in the special built-in window meant to allow cooling during the drilling process and good visualization for correct implant positioning. This happens because the tapered and cylindrical surfaces are partially interrupted, and there are also sharp edges, which are concentrators of forces and stresses.

The area of maximum stress is red (Figure 7a), then, as the stress decreases, the areas are orange, yellow, green, up to dark blue, which are the least stressed. Figure 7b shows the displacements of the guide as red, orange, and yellow areas, but their maximum value is 0.002 mm. This does not influence the movement of the guide fixed on the teeth or the diameter of the guide main hole, which would thus produce additional contact with the drill shank. Figure 7c,d show how displacements propagate. Thus, a more pronounced propagation (orange color) is observed on the thinner wall of the guide with a flat surface (light blue color in Figure 7d). Additionally, in Figure 7c, it is noted that the guide has a small tendency to move from the neighboring tooth (right), but the value is very small and insignificant.

The FEA has an accuracy of 12.4%, which is quite good. In FEA practice, if the results have errors between 0% (theoretical) and 15%, then they can be accepted because the simulation is very close to the real case. The Global Error Rate value is determined and displayed by an integrated sensor of the finite element analysis within the CATIA v5 program. Its value is, of course, determined by the level of mesh refinement of the guide model. However, beyond a certain level, additional refinement will not lead to more accurate results; the FEA will take longer and involve important computing resources. Some specialists consider the acceptable error to be up to 5%, 10%, or 20%, depending on the industrial/research field in which FEA is applied and the size and applicability of the part/assembly studied [33–36].

4. Discussion

The present study aimed to evaluate surgical guides without metal sleeves and, simulate, with the aid of FEA, the use of such a dentally supported guide for dental implant insertion in the mandible. The mandible bone was selected due to its highest density [37,38] and, consequently, due to its highest required drilling force.

The digitally designed surgical guide transposes the planned 3D implant position to the surgical field; the perfect fit of the guide on the remaining teeth and the presence of the guiding cylinders (sleeves) play an important role in achieving this purpose. In fully guided surgery, the sleeves can either be acrylic, incorporated into the guide design, or metallic prefabricated sleeves, attached to the custom-fit guide [14]. The use of the surgical guides in daily practice ensures accurate implant placement, increases the probability of successful treatment outcomes, allows predictable flapless surgery and immediate loading, and reduces the risk for technical and biological complications [13,39,40]. However, static implant-guided surgery is not without possible risks related to deviations between the planned implant position and the final clinical outcome [41]. One of the major risks of inaccuracy is guide fracture during drilling for implant bed preparation. In a systematic review of complications associated with guided implant surgery, Voulgarakis et al. identified the fracture of the surgical guide as a common intraoperative complication, with an incidence rate between 6.7% and 9.7% [41].

The fully resin surgical guide became a major trend in the last few years due to its advantages, such as easier customization, even in the posterior dental arch with less interdental space, low manufacturing cost, and great accessibility without jeopardizing implants insertion accuracy [13].

In spite of the great number of clinical studies performed on resin guides for dental implant insertion, a limited number of studies analyzed the behavior of the surgical guide during its use for implant bed preparation [17,18,42,43] and none investigated the behavior of a tooth-supported, extensively used guide. Among the published studies, one evaluated a resin guide for the insertion of a mini implant aiming to restore a central maxillary incisor [18]. The authors proposed a guide with an open-frame design, customized for

use in restoring the anterior maxilla. The performed FEA revealed the fact that maximum equivalent stress was recorded at the junction between the guide support and the guide base, and the maximum displacement (with a value of 0.297 mm) occurred in the area of the guide cylinder [18], which is different from the present study, mainly due to the different design of the guide but also to the way in which it was loaded. The more robust guide used in our study had a considerably lower maximum displacement (0.002 mm), Figure 7b–d illustrating the localization of the maximum displacement and its propagation.

Another study by Miljanovic et al. [17] performed a FEA analysis using ANSYS Workbench software on a surgical guide for mandibular reconstruction with integrated implants. The guide was designed using Blue Sky Plan 4 software, and the guide support was dental solely on the mesial side, the mucosal distal support not being considered. The resin guide was proven to withstand the forces occurring during the surgery. The maximum deformation was registered at the distal part of the drill cylinder, and von Mises stress was the highest in the area of the tooth adjacent to the sleeve, as could be expected [17].

Liu et al. [43] investigated, using FEA with Ansys 5.0 software and experimental simulation, the temperature distribution in the drilling site when preparing for dental implant placement with a surgical guide. They concluded that, to avoid bone overheating, improved cooling methods are required and the drill should be regularly withdrawn during drilling. Moreover, with the use of metallic sleeves, the risk of overheating the bone during drilling increases due to inadequate saline irrigation [15].

Arora et al. proposed a new design of a surgical guide for avoiding increasing temperature during the drilling process and allowing the irrigation flow to reach the drill during osteotomy [42]. A FEA was carried out with the aim of anticipating the temperature in the bone while drilling but applying PMMA properties instead of bone characteristics. The authors claimed that for the new guide design, the circulation of irrigation is better in comparison to the conventional design [42]. However, the surgical guide analyzed in our study has a built-in window to allow cooling during the drilling process. This type of guide design has been successfully used in many clinical cases, without the risk of bone necrosis due to overheating during osteotomy bed preparation when the recommended protocol was followed [3–5,8]. Despite the fact that the areas with maximum stresses appear at the built-in window, the von Mises stress did not exceed 6.92 MPa, far below the risk of resin guide brakeage (failure). However, when the guide design needs to be modified, in some clinical cases due to a lesser mesio-distal space, the custom reduction of the guiding cylinder needs to be performed with caution due to the risk of exceeding stress during drilling and, consequently, surgical guide brakeage.

Recent research [42,44–46] confirms the importance of studying the behavior of the guide through simulation and real tests and brings valuable results regarding the values of the forces and moments that load the guide and the mandible bone in the drilling process. Most authors propose certain values for these loads depending on some conditions, obtain results, and draw conclusions that surgeons should take into account in their practical work in dental clinics.

For the FEA analysis, the data are typically recorded in .stl files, a format original to 3D printing technology in which only the 3D surface geometry is described in a triangular mesh. Generally, the .stl mesh guides the construction of the geometric model, but not the FEA mesh, since it does not have sufficient data and consistency, complexity is too high, and/or is characterized by triangles with compromised edges, missing faces, or an incorrect orientation, self-intersecting mesh elements, e.g., It is well known that a finer mesh results in a more accurate solution. However, using the finest mesh in the whole model is usually a bad strategy because unnecessary calculations will be performed, producing a useless computational cost. The mesh convergence study enables the acquisition of a mesh that satisfactorily balances accuracy and rationalization of computing resources [47].

Thus, the 3D model of the guide must be verified, simplified, and optimized, as we did in our study, to be easily transferred to the complex stages of finite element analysis. The guide was designed as .stl file with a great number of triangles (82,180). With such a

large number of triangles, the analysis with finite elements could not have been carried out on our computers; the complexity of the model would have been too high and unnecessary, it would probably have introduced geometry errors in the later stages of the analysis. After the simplification stage (reduction to 2818 triangles with the Simplification tool), no significant differences in area or volume are observed in the guide model. Simplifying complex models is a common and recommended practice. Of course, if, during the analysis, some limit values appear that can influence the results and conclusions, the user should run a new simplification using another accuracy factor. In the application presented in the paper, the accuracy factor has a value of 0.5 (as can be seen in the video at minute 8.06 [26]).

The 3D model was discretized using a minimum mesh size of 0.5 mm with an absolute sag of 0.2 mm. The mesh of the surgical guide was composed of 90,217 finite elements (tetrahedrons), connected by 145,237 nodes. In certain cases, depending on the characteristics of the analyzed object, some areas of the model can be discretized locally using a larger number of finite elements, but in our case, this was not necessary considering the size and purpose of the guide model. Therefore, taking into account the number of finite elements and nodes presented above, the discretization of the guide model was considered sufficient [30,47].

The analysis was also prepared carefully; many important aspects related to the restraints and loads applied to the solid 3D model of the guide were taken into account. Using adapted relations from the specialized literature and parameters and coefficients recommended and experimentally determined, the finite element analysis in the present study was successfully concluded.

A low error rate and correct results are observed, similar to those presented in other specialized papers but also identified in clinical practice [48].

The analysis determines the most stressed areas of the guide under the action of the established loads and confirms the possibility of breaking some parts of it when the guide shows manufacturing defects and/or the parameters recommended for the mandible bone drilling process are not respected.

The present study has some limitations: only a tooth-supported guide was analyzed for a single implant insertion. Further FEA needs to be performed for more complex surgical guides and for mucosal and mixed (teeth-mucosal) types of support.

5. Conclusions

Taking into consideration the limits of the current research, the designed tooth-supported surgical guide can withstand the forces occurring during the surgery, even in denser bone, without the risk of fracture.

However, when the mesio-distal space between neighboring teeth is limited, the reduction of the wall thickness of the guiding cylinder needs to be undertaken with caution to avoid failure, especially in the built-in window area, since this is the area of maximum stress.

The obtained results need to be interpreted with caution since FEA is a computerized in vitro study in which clinical conditions may not be completely replicated.

Supplementary Materials: The following supporting video tutorial is available at: https://www.youtube.com/watch?v=H6_XfjD3yqs.

Author Contributions: Conceptualization, I.G.G., O.E.B.V. and C.M.C.; methodology, I.G.G., M.D., A.M.C., I.C.S. and C.M.C.; software, I.G.G., C.B. and C.M.C.; validation, O.E.B.V., I.C.S. and I.G.G.; formal analysis, M.D. and I.G.G.; investigation, A.M.C. and O.E.B.V.; resources, C.M.C.; data curation, I.G.G.; writing—original draft preparation, C.M.C., I.G.G. and O.E.B.V.; writing—review and editing, C.M.C. and C.B.; visualization, I.G.G.; supervision, I.C.S.; project administration, C.M.C.; funding acquisition, C.M.C. All authors have read and agreed to the published version of the manuscript.

Funding: I.C. Stancu received funding from the Executive Agency for Higher Education, Research, Development and Innovation Funding, UEFISCDI, project PN-III-P4-PCE-2021-1240, Integrating mechanically-tunable 3D printing with new bioactive multi(nano)materials for next functional personalized bone regenerative scaffolds, PCE88/2022, Next3DBone.

Institutional Review Board Statement: Not applicable.

Informed Consent Statement: Not applicable.

Data Availability Statement: Supplementary Materials are available on request from the corresponding authors.

Conflicts of Interest: The authors declare no conflict of interest. Cristian Butnărașu is a collaborator, not an employee, of Megagen Dental Laboratory in Bucharest, Romania.

References

- Costa, A.J.d.M.; Teixeira Neto, A.D.; Burgoa, S.; Gutierrez, V.; Cortes, A.R.G. Fully Digital Workflow with Magnetically Connected Guides for Full-Arch Implant Rehabilitation Following Guided Alveolar Ridge Reduction. *J. Prosthodont.* **2020**, *29*, 272–276. [\[CrossRef\]](#)
- Iorgulescu, G.; Cristache, C.M.; Burcea, C.C.; Ionescu, I.; Perieanu, V.S.; Marcov, N.; Burlibasa, M. Ethical and medico-legal aspects behind the use of digital technologies in dentistry. *Rom. J. Leg. Med.* **2020**, *28*, 202–207. [\[CrossRef\]](#)
- Chandran, S.; Sers, L.; Picciocchi, G.; Luongo, F.; Lerner, H.; Engelschalk, M.; Omar, S. Guided implant surgery with R2Gate®: A multicenter retrospective clinical study with 1 year of follow-up. *J. Dent.* **2022**, *127*, 104349. [\[CrossRef\]](#)
- Cristache, C.M. Presurgical Cone Beam Computed Tomography Bone Quality Evaluation for Predictable Immediate Implant Placement and Restoration in Esthetic Zone. *Case Rep. Dent.* **2017**, *2017*, 1096365. [\[CrossRef\]](#) [\[PubMed\]](#)
- Cristache, C.M.; Burlibasa, M.; Tudor, I.; Totu, E.E.; Di Francesco, F.; Moraru, L. Accuracy, Labor-Time and Patient-Reported Outcomes with Partially versus Fully Digital Workflow for Flapless Guided Dental Implants Insertion—A Randomized Clinical Trial with One-Year Follow-Up. *J. Clin. Med.* **2021**, *10*, 1102. [\[CrossRef\]](#) [\[PubMed\]](#)
- Zhan, Y.; Wang, M.; Cheng, X.; Li, Y.; Shi, X.; Liu, F. Evaluation of a dynamic navigation system for training students in dental implant placement. *J. Dent. Educ.* **2021**, *85*, 120–127. [\[CrossRef\]](#) [\[PubMed\]](#)
- Spille, J.; Helmstetter, E.; Kübel, P.; Weitkamp, J.-T.; Wagner, J.; Wieker, H.; Naujokat, H.; Flörke, C.; Wiltfang, J.; Gülses, A. Learning Curve and Comparison of Dynamic Implant Placement Accuracy Using a Navigation System in Young Professionals. *Dent. J.* **2022**, *10*, 187. [\[CrossRef\]](#)
- Cristache, C.M.; Gurbanescu, S. Accuracy Evaluation of a Stereolithographic Surgical Template for Dental Implant Insertion Using 3D Superimposition Protocol. *Int. J. Dent.* **2017**, *2017*, 4292081. [\[CrossRef\]](#)
- Oh, K.C.; Shim, J.S.; Park, J.M. In Vitro Comparison between Metal Sleeve-Free and Metal Sleeve-Incorporated 3D-Printed Computer-Assisted Implant Surgical Guides. *Materials* **2021**, *14*, 615. [\[CrossRef\]](#)
- Schneider, D.; Schober, F.; Grohmann, P.; Hammerle, C.H.F.; Jung, R.E. In-vitro evaluation of the tolerance of surgical instruments in templates for computer-assisted guided implantology produced by 3-D printing. *Clin. Oral Implant. Res.* **2015**, *26*, 320–325. [\[CrossRef\]](#)
- Oh, K.C.; Park, J.M.; Shim, J.S.; Kim, J.H.; Kim, J.E.; Kim, J.H. Assessment of metal sleeve-free 3D-printed implant surgical guides. *Dent. Mater.* **2019**, *35*, 468–476. [\[CrossRef\]](#) [\[PubMed\]](#)
- Elkomy, M.M.; Khamis, M.M.; El-Sharkawy, A.M. Clinical and radiographic evaluation of implants placed with fully guided versus partially guided tissue-supported surgical guides: A split-mouth clinical study. *J. Prosthet. Dent.* **2021**, *126*, 58–66. [\[CrossRef\]](#) [\[PubMed\]](#)
- Tallarico, M.; Czajkowska, M.; Cicciù, M.; Giardina, F.; Minciarelli, A.; Zadrożny, Ł.; Park, C.-J.; Meloni, S.M. Accuracy of surgical templates with and without metallic sleeves in case of partial arch restorations: A systematic review. *J. Dent.* **2021**, *115*, 300–5712. [\[CrossRef\]](#)
- Tallarico, M.; Martinolli, M.; Kim, Y.J.; Cocchi, F.; Meloni, S.M.; Alushi, A.; Xhanari, E. Accuracy of Computer-Assisted Template-Based Implant Placement Using Two Different Surgical Templates Designed with or without Metallic Sleeves: A Randomized Controlled Trial. *Dent. J.* **2019**, *7*, 41. [\[CrossRef\]](#)
- Kalaivani, G.; Balaji, V.R.; Manikandan, D.; Rohini, G. Expectation and reality of guided implant surgery protocol using computer-assisted static and dynamic navigation system at present scenario: Evidence-based literature review. *J. Indian Soc. Periodontol.* **2020**, *24*, 398–408. [\[CrossRef\]](#) [\[PubMed\]](#)
- Hultin, M.; Svensson, K.G.; Trulsson, M. Clinical advantages of computer-guided implant placement: A systematic review. *Clin. Oral Implant. Res.* **2012**, *23* (Suppl. S6), 124–135. [\[CrossRef\]](#)
- Miljanovic, D.; Seyedmahmoudian, M.; Horan, B.; Stojcevski, A. Novel and accurate 3D-Printed surgical guide for mandibular reconstruction with integrated dental implants. *Comput. Biol. Med.* **2022**, *151*, 106327. [\[CrossRef\]](#)
- Nagib, R.; Farkas, A.Z.; Szuhaneck, C. FEM Analysis of Individualized Polymeric 3D Printed Guide for Orthodontic Mini-Implant Insertion as Temporary Crown Support in the Anterior Maxillary Area. *Polymers* **2023**, *15*, 879. [\[CrossRef\]](#)

19. Bandela, V.; Kanaparthi, S. *Finite Element Analysis and Its Applications in Dentistry*; Baccouch, M., Ed.; IntechOpen: Rijeka, Croatia, 2020; Chapter 8, ISBN 978-1-83962-342-4.
20. Reddy, M.S.; Sundram, R.; Eid Abdemagyd, H.A. Application of Finite Element Model in Implant Dentistry: A Systematic Review. *J. Pharm. Bioallied Sci.* **2019**, *11*, S85. [[CrossRef](#)]
21. Mukai, S.; Mukai, E.; Santos-Junior, J.A.; Shibli, J.A.; Faveri, M.; Giro, G. Assessment of the reproducibility and precision of milling and 3D printing surgical guides. *BMC Oral Health* **2021**, *21*, 1. [[CrossRef](#)]
22. Son, K.; Lee, K.B. A novel method for precise guided hole fabrication of dental implant surgical guide fabricated with 3d printing technology. *Appl. Sci.* **2021**, *11*, 49. [[CrossRef](#)]
23. Yamakawa, S.; Shimada, K. Removing Self Intersections of a Triangular Mesh by Edge Swapping, Edge Hammering, and Face Lifting. In Proceedings of the 18th International Meshing Roundtable, Salt Lake City, UT, USA, 25–28 October 2009; Clark, B.W., Ed.; Springer: Berlin/Heidelberg, Germany, 2009; pp. 13–29.
24. Cignoni, P.; Callieri, M.; Corsini, M.; Dellepiane, M.; Ganovelli, F.; Ranzuglia, G. Meshlab: An open-source mesh processing tool. In Proceedings of the Eurographics Italian Chapter Conference, Salerno, Italy, 2–4 July 2008; Volume 2008, pp. 129–136.
25. Leordean, D.; Vilău, C.; Dulescu, M.C. Generation of Computational 3D Models of Human Bones Based on STL Data and CAD Software Packages. *Appl. Sci.* **2021**, *11*, 7964. [[CrossRef](#)]
26. Ghionea, I.-G. CATIA v5 How to Transform a STL Surface into a Solid Model—YouTube. Available online: https://www.youtube.com/watch?v=H6_XfjD3yqs (accessed on 15 August 2023).
27. Dechow, P.C.; Nail, G.A.; Schwartz-Dabney, C.L.; Ashman, R.B. Elastic properties of human supraorbital and mandibular bone. *Am. J. Phys. Anthropol.* **1993**, *90*, 291–306. [[CrossRef](#)] [[PubMed](#)]
28. Lakatos, É.; Magyar, L.; Bojtár, I. Material Properties of the Mandibular Trabecular Bone. *J. Med. Eng.* **2014**, *2014*, 470539. [[CrossRef](#)] [[PubMed](#)]
29. Odin, G.; Savoldelli, C.; Bouchard, P.-O.; Tillier, Y. Determination of Young’s modulus of mandibular bone using inverse analysis. *Med. Eng. Phys.* **2010**, *32*, 630–637. [[CrossRef](#)] [[PubMed](#)]
30. Gröning, F.; Bright, J.A.; Fagan, M.J.; O’Higgins, P. Improving the validation of finite element models with quantitative full-field strain comparisons. *J. Biomech.* **2012**, *45*, 1498–1506. [[CrossRef](#)]
31. Picos, C.; Pruteanu, O.; Bohosievici, C.; Coman, G.; Braha, V.; Paraschiv, D.; Slatineanu, L.; Gramescu, T. *Proiectarea Tehnologiiilor de Prelucrarea Mecanica Prin Aschiere: Manual de Proiectare*; Chisinau University Publishing House: Chisinau, Moldova, 1992; Volume 2, ISBN 5-362-00971-0.
32. Vlase, A. *Tehnologia Constructiilor de Masini*; Editura Tehnică: Bucharest, Romania, 1996; ISBN 973-31-0777-8.
33. Rahman, H.A.; Khairi, N.D.A.; Sani, M.S.M. Finite Element Model Updating of Dissimilar Plate with Rivet Joint. *J. Phys. Conf. Ser.* **2019**, *1262*, 012035. [[CrossRef](#)]
34. Federal Aviation Administration Finite Element Modeling and Analysis Validation Finite Element Analysis Validation Requirements and Methods Terminal Objectives. Available online: <https://appliedcax.com/docs/femap/femap-symposium-2015-seattle-area/FEA-Validation-Requirements-and-Methods-Final-with-Transcript.pdf> (accessed on 31 August 2023).
35. How to Interpret FEA Results?—Enterfea. Available online: <https://enterfea.com/how-to-interpret-fea-results/> (accessed on 31 August 2023).
36. Mohanty, R.K.; Mohanty, R.C.; Sabut, S.K. Finite element analysis and experimental validation of polycentric prosthetic knee. *Mater. Today Proc.* **2022**, *63*, 207–214. [[CrossRef](#)]
37. Shemtov-Yona, K. Quantitative assessment of the jawbone quality classification: A meta-analysis study. *PLoS ONE* **2021**, *16*, e0253283. [[CrossRef](#)]
38. Chatvaratthana, K.; Thaworanunta, S.; Seriwatanachai, D.; Wongsirichat, N. Correlation between the thickness of the crestal and buccolingual cortical bone at varying depths and implant stability quotients. *PLoS ONE* **2017**, *12*, e0190293. [[CrossRef](#)]
39. Tahmaseb, A.; Wu, V.; Wismeijer, D.; Coucke, W.; Evans, C. The accuracy of static computer-aided implant surgery: A systematic review and meta-analysis. *Clin. Oral Implant. Res.* **2018**, *29*, 416–435. [[CrossRef](#)] [[PubMed](#)]
40. Park, J.Y.; Song, Y.W.; Park, S.H.; Kim, J.H.; Park, J.M.; Lee, J.S. Clinical factors influencing implant positioning by guided surgery using a nonmetal sleeve template in the partially edentulous ridge: Multiple regression analysis of a prospective cohort. *Clin. Oral Implant. Res.* **2020**, *31*, 1187–1198. [[CrossRef](#)]
41. Voulgarakis, A.; Strub, J.R.; Att, W. Outcomes of implants placed with three different flapless surgical procedures: A systematic review. *Int. J. Oral Maxillofac. Surg.* **2014**, *43*, 476–486. [[CrossRef](#)] [[PubMed](#)]
42. Arora, V.; Kumar, S.; Kalra, P.; Goyal, A. Finite element analysis of dental implant surgical guides. *Mater. Today Proc.* **2022**, *56*, 3137–3141. [[CrossRef](#)]
43. Liu, Y.F.; Wu, J.L.; Zhang, J.X.; Peng, W.; Liao, W.Q. Numerical and Experimental Analyses on the Temperature Distribution in the Dental Implant Preparation Area when Using a Surgical Guide. *J. Prosthodont.* **2018**, *27*, 42–51. [[CrossRef](#)] [[PubMed](#)]
44. Goswami, M.M.; Kumar, M.; Vats, A.; Bansal, A.S. Evaluation of dental implant insertion torque using a manual ratchet. *Med. J. Armed Forces India* **2015**, *71*, S327–S332. [[CrossRef](#)]
45. Li, L.; Zhang, S.; Li, Q.; Bian, C.; Zhang, A. Oblique Cutting Based Mechanical Model for Insertion Torque of Dental Implant. *Chin. J. Mech. Eng.* **2022**, *35*, 56. [[CrossRef](#)]
46. Hada, T.; Kanazawa, M.; Iwaki, M.; Katheng, A.; Minakuchi, S. Comparison of Mechanical Properties of PMMA Disks for Digitally Designed Dentures. *Polymers* **2021**, *13*, 1745. [[CrossRef](#)]

47. Meira, J.B.C.; Jikihara, A.N.; Capetillo, P.; Roscoe, M.G.; Cattaneo, P.M.; Ballester, R.Y. Finite element analysis in dentistry. In *Dental Biomaterials*; World Scientific Publishing Co. Pte Ltd.: 5 Toh Tuck Link, Singapore, 2019; pp. 67–89, ISBN 2529-816X.
48. Vadiraj, B.; Rao, P.K.V.; Kiran Kumar, K. Application of biomaterials and finite element analysis in dentistry—A review. *Mater. Today Proc.* **2023**, *76*, 564–568. [[CrossRef](#)]

Disclaimer/Publisher’s Note: The statements, opinions and data contained in all publications are solely those of the individual author(s) and contributor(s) and not of MDPI and/or the editor(s). MDPI and/or the editor(s) disclaim responsibility for any injury to people or property resulting from any ideas, methods, instructions or products referred to in the content.